

# Preliminary determination of angular distribution of neutrons emitted from PF-1000 facility by indium activation

Sławomir Jednoróg,  
Adam Szydłowski,  
Marek Scholz,  
Marian Paduch,  
Barbara Bienkowska

**Abstract.** This paper presents a new method applied to measure the angular neutron emission from Plasma Focus (PF) – type deuterium discharges performed within the PF-1000 facility. Neutrons were recorded by activation of especially optimized (mass and shape) indium samples with subsequent gamma spectrometry to measure the induced activity of the samples. The neutron fluence rate on every indium sample used was determined using neutron transport calculation and measured activity of the samples.

**Key words:** plasma focus • neutron activation technique • plasma diagnostics

## Introduction

Many high-temperature plasma experimental devices, and among them plasma-focus (PF) facilities, have reach a level of operation at which intense fluxes of fast neutrons are emitted. The mega-joule PF fusion experiments involving deuterium plasma with ion temperature exceeding 1 keV, deuterium densities equal to a few  $10^{19} \text{ cm}^{-3}$ , plasma volume of a few  $\text{cm}^3$ , and plasma lifetime of  $200 \div 300 \text{ ns}$ , generates a few  $10^{11}$  or more neutrons per shot. At this level of emission it will be feasible to extract information about plasma parameters by making use of various techniques measuring neutron yield and energy distribution of these and other fusion products.

Mechanisms of the neutron emission from pinched plasma discharges still remain unclear. In spite of many efforts, both theoretical and experimental, the problem of the prevailing mechanism of the interaction between two deuterium reagents leading to fusion reactions has not been solved. At the aforementioned neutron emission levels it could be possible to obtain information about distributions of the plasma  $\text{D}^+$ -ions (nuclear reaction reagents) using suitable neutron diagnostic techniques. Neutron activation is one of the methods that is widely used to determine the neutron fluence at points of interest and is well suited for precisely measuring the neutron yield [2]. The advantages of this method are; its immunity to electromagnetic interferences and it secures a large dynamic range of the measurements. Information about neutron fluence is received by registering the products of nuclear reactions induced in samples of especially selected materials. The materials are selected so that they have relatively

S. Jednoróg✉, M. Scholz, M. Paduch, B. Bienkowska  
Division of Magnetised Plasma,  
Institute of Plasma Physics and Laser Microfusion,  
Association EURATOM,  
23 Hery Str., 01-497 Warsaw, Poland,  
Tel.: +48 22 638 1005 ext. 63, Fax: +48 22 666 8372,  
E-mail: jednorog@ifpilm.waw.pl

A. Szydłowski  
Department of Plasma Physics and Material  
Engineering,  
National Centre for Nuclear Research (NCBJ),  
Association EURATOM,  
7 Andrzeja Sołtana Str., 05-400 Otwock/Świerk, Poland

Received: 11 September 2011

Accepted: 20 January 2012

high reaction cross-sections for neutrons, well defined nuclear reaction thresholds and the products of these reactions decay with half-lives in the range of a few seconds or longer. Usually, the products decay with gamma-ray emission and can thus be detected using gamma spectrometry. The measured gamma activity of the sample (i.e. reaction rate) is converted into the neutron fluence at selected locations around the pinch plasma using neutron transport calculations Monte Carlo n-particle (MCNP) [3].

The anisotropy of neutron fluxes from D-D reactions occurring in Plasma Focus discharges was reported in many papers which were published during the 1970s, 1980s, and also 1990s [1, 6–9, 15]. It was generally assigned to the axial beam-target mechanism, whereby the beams were generated by strong electric fields associated with  $m = 0$  instability zones. The flux anisotropy comes from both the center of mass motion of the reagents and the angular dependence of the differential D-D reaction cross-section in the target model. Measurements of the angular dependent neutron fluxes were generally made by the use of silver activation counters. However, to measure such short neutron pulses thoroughly the detectors which are used must preserve the fluence information for analysis after discharge. The decay of the neutron induced reaction products must be distinct from the background and directly related to the incident neutron intensity. It seems that the silver activation detectors do not achieve all these requirements, in spite of the fact that they have been used for many years to measure neutron fluence from many pulsed sources. These instruments consist of a silver foil wrapped around a Geiger-Müller (G-M) tube. Recorded neutrons are first slowed down in a hydrogenous moderator and after that captured in the silver by the two reactions;  $^{107}\text{Ag}(n,\gamma)^{108}\text{Ag}$  and  $^{109}\text{Ag}(n,\gamma)^{110}\text{Ag}$ . Subsequent beta decay of the activation products is counted with the G-M tube. The main drawback of this instrument is that it is excessively sensitive to scattered neutrons. The scattered and slowed down neutron field constitutes a serious problem for neutron measurements in many high temperature plasma experiments. The results of some neutron measurements are effectively influenced by the background of slowed down neutrons.

The method based on the threshold nuclear reaction with indium is demonstrated in this paper. This method has been already successfully harnessed for large tokamak experiments like JET [12]. The results of measurements of angular distribution of neutrons emitted from a dozens of PF-1000 facility discharges, which were performed with the newly introduced indium monitor, are presented.

### Experimental arrangements

The PF-1000 device is a Mather-type facility [13, 14, 16]. It is equipped with two coaxial electrodes of the same length (460 mm). The inner electrode (anode) is made of copper (diameter – 230 mm). The outer electrode (cathode, diameter – 400 mm) consists of 12 stainless steel tubes (diameter – 80 mm). The anode is surrounded tightly by a cylindrical, ceramic insulator (length – 85 mm). The

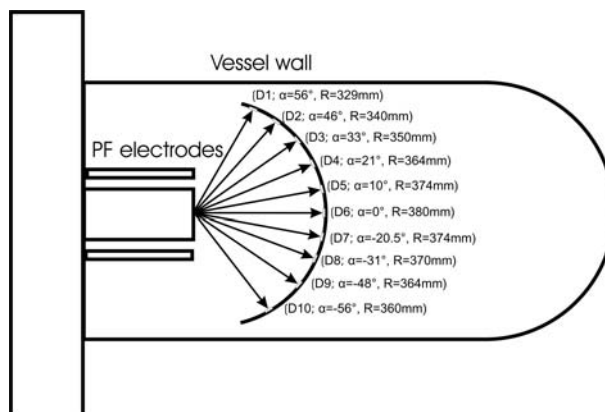


**Fig. 1.** Layout of ten indium sample inside the PF-1000 facility vacuum vessel. The activation of light samples allow to determinate angular distribution of neutrons.

experiment has been performed in a vacuum chamber pumped out to the basic pressure of  $2 \times 10^{-5}$  hPa. The deuterium filling has been varied, for different discharges, in the range of 1.6–1.8 hPa. In most discharges the capacitor bank, capable of accumulating 1064 kJ energy at 40 kV, was charged to 24–25 kV.

The measurements were carried out in two different sample configurations. In the first configuration 10 small indium samples ( $5 \times 20$  mm) were used. All the samples were located inside a PF-1000 vacuum vessel. They were attached to a semicircular support at a distance of 35 cm from the inner electrode face and each of them was inserted at a different angle to the electrode axis (Fig. 1). The samples were exposed to neutrons emitted from a series of 10 PF-1000 discharges. After the irradiation, they were removed from the vessel and gamma-rays emitted by each sample were measured using a cross-calibrated NaI scintillation probe.

In the second configuration a set of larger indium samples was used. These samples were located on the vacuum vessel outer walls, in the plane parallel to the axis of the inner electrodes and each sample at a different angle with respect to the electrode axis (Fig. 2). The experiments were performed in two variants: first, with the sample D9 (Fig. 2) placed directly on the vessel's

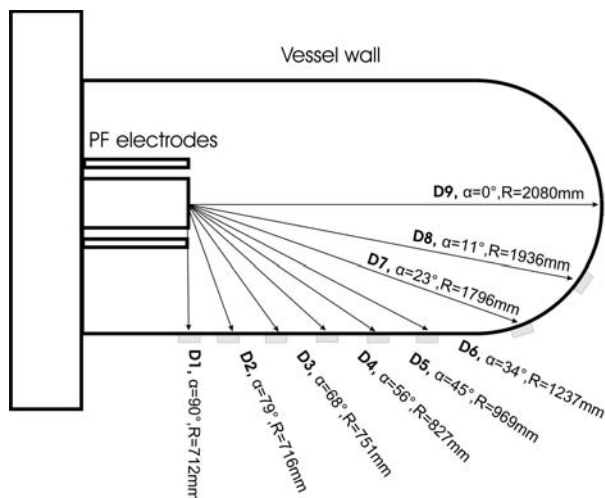


**Fig. 2.** Layout of indium samples on the outer surface of the vacuum chamber walls. The configuration of nine large indium samples allows identification of angular distribution of neutrons by measurement of nuclear reactions caused by neutrons.

**Table 1.** Threshold nuclear reactions occurring during activation of indium samples by neutrons [10]

Target nucleus	Nuclear reaction	Product nucleus	Threshold (MeV)	Cross-section for 2.45 MeV (b)	Product ( $T_{1/2}$ )	Daughter nucleus	$\gamma$ energy (keV)	Intensity (%)
$^{113}\text{In}$	n,2n	$^{112}\text{In}$	10.00	0.00E+00	14.97 m	$^{112}\text{Cd}$	606.40	1.11
$^{113}\text{In}$	n,2n	$^{112}\text{In}$	11.00	0.00E+00	14.97 m	$^{112}\text{Cd}$	617.10	4.60
$^{113}\text{In}$	n,2n	$^{112}\text{In}$	12.00	0.00E+00	20.56 m	$^{112}\text{In}$	156.40	13.20
$^{113}\text{In}$	n,2n	$^{112}\text{In}$	13.00	0.00E+00	14.97 m	$^{112}\text{Cd}$	511.00	42.00
$^{113}\text{In}$	<b>n,n'</b>	<b><math>^{112}\text{In}</math></b>	<b>0.40</b>	<b>1.53E+00</b>	<b>99.476 m</b>	<b><math>^{113}\text{In}</math></b>	<b>391.70</b>	<b>64.94</b>
$^{113}\text{In}$	n,p	$^{113}\text{Cd}$	0.50	2.23E-12	stable			
$^{113}\text{In}$	n,d	$^{112}\text{Cd}$	6.00	0.00E+00	stable			
$^{115}\text{In}$	n,2n	$^{114}\text{In}$	0.60	2.93E-02	49.51 d	$^{114}\text{Cd}$	558.43	3.20
$^{115}\text{In}$	n,2n	$^{114}\text{In}$	1.60	2.93E-02	49.51 d	$^{114}\text{Cd}$	725.24	3.20
$^{115}\text{In}$	n,2n	$^{114}\text{In}$	2.60	2.93E-02	49.51 d	$^{114}\text{In}$	190.27	15.56
$^{115}\text{In}$	n,p	$^{115}\text{Cd}$	2.00	< 7.55E-16	53.46 h	$^{115}\text{In}$	260.90	1.94
$^{115}\text{In}$	n,p	$^{115}\text{Cd}$	2.00	< 7.55E-16	44.56 d	$^{115}\text{In}$	933.84	2.00
$^{115}\text{In}$	n,p	$^{115}\text{Cd}$	2.00	< 7.55E-16	53.46 h	$^{115}\text{In}$	492.35	8.03
$^{115}\text{In}$	n,p	$^{115}\text{Cd}$	2.00	< 7.55E-16	53.46 h	$^{115}\text{In}$	527.90	27.50
$^{115}\text{In}$	n,p	$^{115}\text{Cd}$	2.00	< 7.55E-16	53.46 h	$^{115}\text{In}$	336.24	45.90
$^{115}\text{In}$	n,d	$^{114}\text{Cd}$	6.87	0.00E+00	stable			
$^{115}\text{In}$	<b>n,n'</b>	<b><math>^{115}\text{In}</math></b>	<b>0.34</b>	<b>1.58E+00</b>	<b>4.486 h</b>	<b><math>^{115}\text{In}</math></b>	<b>336.24</b>	<b>45.80</b>

wall and second, the sample was placed on a special holder which was introduced to the vacuum vessel to bring the samples closer to the main PF electrode.

### Monitoring of neutrons, based on nuclear reactions with indium and gamma spectroscopy

The threshold nuclear reactions occurring in indium during activation by neutrons are shown in Table 1. Only two highlighted reactions are useful for measurements of neutrons emitted from PF-1000 facility discharges. The threshold of these reactions is below 2.45 MeV and the cross-section is high enough. The nuclear reaction  $^{115}\text{In}(n,n')$  is the most important among other reactions because its occurrence is most likely due to the dominant abundance of this isotope (95.71%) inside the mixture of stable indium isotopes. In the case of  $^{115\text{m}}\text{In}$  the detection of photons with an energy of 336 keV reveals the presence of neutrons with energies above  $\sim 340$  keV.

The semiconductor detection system for gamma ray registration consists of:

- an InSpector 2000 multichannel analyzer (MCA),
- a high purity germanium (HPGe) coaxial detector system with 30% efficiency, FWHM = 1.8 keV for 1332 keV gamma line,
- Genie-2000 Gamma Analysis Software,
- numerical characteristic of the HPGe detector,
- Laboratory Sourceless Object Calibration Software (LabSOCS),
- the shielding system consists of the specially designed electromagnetic shield (EMS) and the typical shield for radiation background reduction.

The HPGe detector with radiation shield, MCA, and a steering computer were placed inside the EMS and supplied with power on uninterruptible power supply. This protects the whole system against electromagnetic interference even propagated throughout the power network.

The HPGe detector has been supplied with its numerical characteristic (NCh) which allows the deter-

mination of the sample activity without performing the efficiency calibration *in situ*. The NCh of the detector was provided by the manufacturer. At the factory, the exact dimensions of this particular detector, including its mounting and housing, were implemented into an MCNP model named LabSOCS. Each detector provided with its own NCh has been also examined with a broad number of calibration sources of different shape, elemental composition and density as well. As stated in [4] and [5], LabSOCS energy-efficiency calibration data-points have a typical accuracy of:  $\sim 7\%$  standard deviation (SD) for energies <150 keV,  $\sim 6\%$  SD for 150–400 keV,  $\sim 4\%$  SD for 400–7000 keV. Our energy-efficiency calibration tests, performed with some certified calibration sources placed in Marinelli geometry, are in good agreement with LabSOCS data. A comparison of both the calibrations, i.e. that performed using a calibration source and calculated one with the LabSOCS, is shown in Fig. 3.

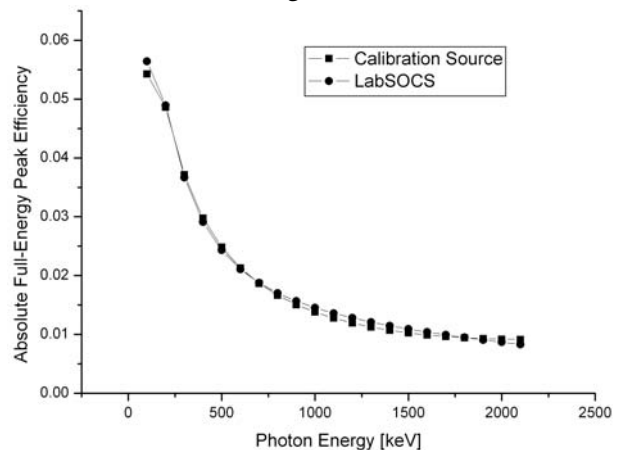


**Fig. 3.** The comparison of two methods of efficiency calibration. Calibration curve with measurement points presented in the form of filled squares (■) shows the AFEPE (absolute-full-energy-peak-efficiency) obtained using a calibration source placed in a Marinelli beaker, while the curve with filled circles (●) represents the efficiency calibrations performed by the LabSOCS (Laboratory Sourceless Calibration Software) mathematical efficiency calibration software.

The reliable detection and identification of the maximum number of nuclear reactions require an optimal sample geometry as well as measurement geometry (i.e. optimization) which ensures both high sample activation and effective registration of photons by means of the HPGe detector. Increasing the mass of the sample leads to an increase in the number of nuclei that can be activated with neutrons. On the other hand, an increasing sample size leads to a decreasing of the efficiency for the registration of gamma quanta. All processes of gamma absorption in the sample for all possible geometries are taken into account by computer software operating with a detector during estimation of particular efficiency.

The Integrated-Mass-Absolute-Full-Energy-Peak-Efficiency is a definite Riemann integral of mass and efficiency product and takes into account both the reactivity of the sample and the efficiency of its measurement by the HPGe detector. Optimization is a process of finding the best sample shape among plenty others, and the biggest sample mass. Fulfilling the above-mentioned criteria, a heavy cylindrical sample with a diameter of 63.7 mm and 4.3 mm in thickness was proposed as the activation sample [11]. The system consists of indium samples, which are optimized in size and shape. The HPGe detector is characterized by a high resolution and the highest efficiency for gamma registration and allows measurements of sample activity in the range even tenth part of Becquerel. This system was applied for the activation of samples outside the vacuum vessel wall. The angular distribution of neutrons was also determined by them. The HPGe detector has been also used for efficiency cross calibration of the BrillanCe probe and for measurement of the large samples. In this way after one PF discharge much more activation samples were measured in shorter time which allowed collection of information before disintegration of the activated nuclei.

The NaI probe with the Tukan MCA was applied mainly for the measurement of small samples (20 mm in diameter and 5 mm in thickness), activated inside the vacuum vessel. However, the mentioned method was also applied to measure the large (described previously) samples activated on the outer wall of the PF-1000 facilities. The energy calibration of spectrometry systems were done with a set of point sources with energy started from 59.54 keV ( $^{241}\text{Am}$ ) up to 1836 keV ( $^{88}\text{Y}$ ). The efficiency calibration of the BrillanCe system was performed by a cross calibration method. One singular sample, which represents both types was taken from the set of samples and after that it was activated with an Am-Be neutron source. Then, the sample was measured with a NaI probe and the HPGe detector, respectively. The activities of  $^{115\text{m}}\text{In}$  and  $^{116}\text{In}$  were both precisely determined with the HPGe spectrometry system. Finally, these results were used to calculate the particular sample efficiencies for the NaI probe. The sample geometry and measurement geometry during cross calibration and experimental procedures were preserved.

### The MCNP geometrical model

The most effort-consuming part of the neutron analysis for calculating the fluence of neutrons in the samples

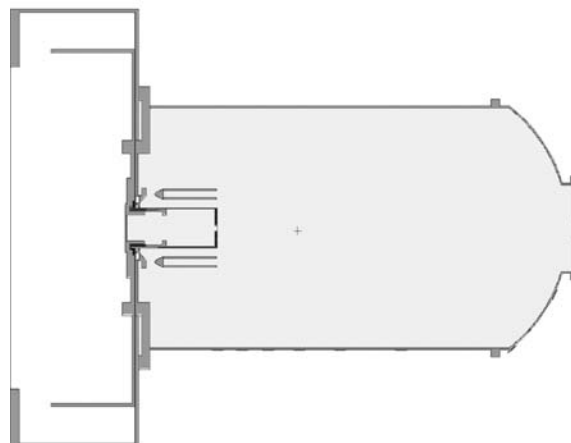


**Fig. 4.** Cut view of geometry from MCNP input.

lies in providing an accurate description of the geometrical and material components of the device in the code. A geometrical model of the PF-1000 facility has been prepared for neutron transport Monte Carlo calculations with the MCNP code. Structure of the steel chamber, steel and copper electrode set and indium samples have been quite accurately modelled. Cut view of the geometry from MCNP input is shown in Fig. 4. The MCNP5 [17] code with MCNP5DATA [18] cross-section library have been used for calculations of neutron distributions outside the chamber of the PF-1000 facility. Monte Carlo simulations have been performed for 2.5 MeV neutrons. It has been assumed that the neutrons were emitted from a point isotropic source, which was placed at different positions of the pinch plasma. The number of simulated histories for each neutron source has been  $2 \times 10^8$ . The estimated relative errors achieved for the calculated results are usually below 1%.

### Results

The results obtained with the set of small indium samples exposed inside the PF-1000 vacuum vessel are presented in Fig. 5. The samples were irradiated with

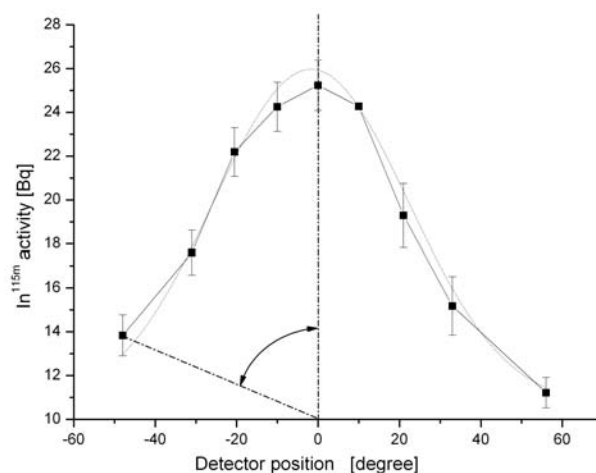


**Fig. 5.** Horizontal distribution of activity induced by neutrons emitted from PF-1000 facilities during row of 10 discharges. Measurements were committed with NaI probe. Note: the distance from the anode plate to indium samples is taken into account in evaluation of the activity. Dot lines represent Gaussian fit of experimental data.

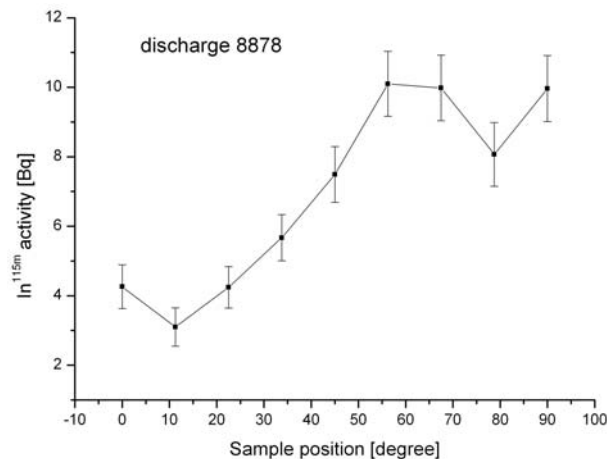


**Fig. 6.** Measured activities of indium samples located at different angles relative to the electrode axis. Note: the distance from the neutron source (plasma pinch) is different for each sample. Discharge 8878 with neutron yield measured by silver activation counter  $Y_n = 3 \times 10^{11}$ .

neutrons emitted from a series of 10 discharges and measured with the NaI probe. The line that connects the measurement points is symmetrical and the results can be well fitted by a Gaussian distribution. Using this configuration, we were able to measure integrated angular distributions of neutrons emitted from a series of 10 discharges.

Using the  $^{115}\text{In}(n,n')^{115\text{m}}\text{In}$  nuclear reaction and the semiconductor detection system, the angular distributions of neutrons were measured for a single PF discharge. The samples were activated on the outer walls or sample holder and after that they were precisely measured with the gamma spectrometer and their initial activities were then calculated. The measurements were performed for discharges with different neutron emissions. The activities of  $^{115\text{m}}\text{In}$  radionuclide changed from tenths of Becquerel up to a few of Becquerel. Those values increased with the neutron emission rate. All the angular distribution curves had a very similar shape. Exemplary result is shown in Fig. 6.

MCNP calculations with a source of D-D neutrons (2.5 MeV) placed at different positions from the PF-1000 anode plate have been performed. Measured and calculated reaction rates for the  $^{115}\text{In}(n,n')^{115\text{m}}\text{In}$  reaction have been used to identify the fluence rate of neutrons in each sample from the following formula:

$$(1) \quad \phi_{\text{exp}} = \phi_{\text{cal}} \cdot \frac{\alpha_{\text{exp}}}{\alpha_{\text{cal}}}$$

where:  $\alpha_{\text{exp}}$  – measured reaction rate,  $\alpha_{\text{cal}}$  – reaction rate calculated from MCNP,  $\phi_{\text{cal}}$  – fluence rate of neutrons calculated from MCNP.

Neutron fluence rate anisotropy at an angle of  $\theta_i$  in relation to the electrode axis has been calculated from the formula:

$$(2) \quad A(\theta_i) = \frac{\phi_{\text{exp}}^0}{\phi_{\text{exp}}^i} \cdot \frac{1}{c_i}$$

where:  $c_i = \phi_{\text{cal}}^0 / \phi_{\text{cal}}^i$  geometrical coefficient calculated from MCNP, determining the influence of surroundings on neutrons emitted at the  $i$ -th angle in relation to the neutrons emitted at an angle of  $0^\circ$ .

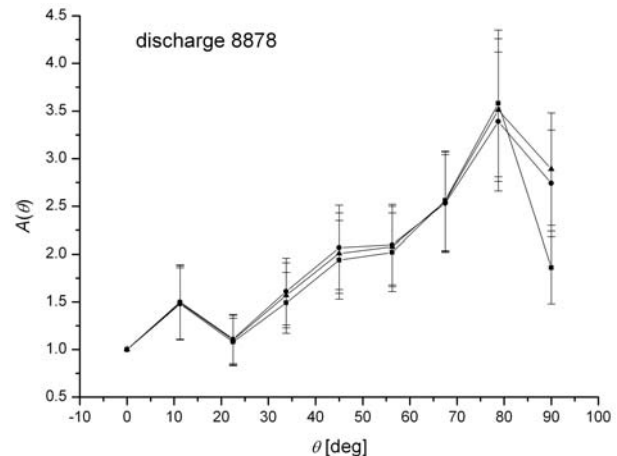


**Fig. 7.** Neutron fluence rate anisotropy evaluated from measurements of samples activity and calculations of  $^{115}\text{In}(n,n')^{115\text{m}}\text{In}$  reaction rate in every sample. Calculations were performed for 3 distances of the point source from the inner electrode end: ■ – 0 cm, ● – 5 cm and ▲ – 10 cm.

Using the results presented in Fig. 6, the neutron fluence rate anisotropy was evaluated. The  $A(\theta)$  calculated from Eq. (2) is shown in Fig. 7. Using neutron fluence rate anisotropy evaluated from the experiment, the character of neutron emission from pinch plasma can be shown. Such high anisotropy coefficient (up to 3.5) confirms the hypothesis that neutrons are produced mostly by intensive beams of fast deuterons, which induce nuclear reactions in the pinched plasma as well as in the gas target filling the discharge chamber.

## Conclusions

The results of the above studies described in this paper can be summarized as follows:

- The angular distributions of 2.5 MeV fusion neutrons emitted from PF-1000 discharges were measured using the activation technique. That research work was oriented to look for a new diagnostic method for studying more precisely the neutron emission characteristic. This can lead to better understanding of the mechanism of neutron generation in PF-1000 discharges.
- Two different ways of neutron emission anisotropy measurements by means of activation technique were applied in the PF experiment: one with the samples near the pinch plasma (inside the PF vacuum chamber) and the second with the samples located far away (on the PF vacuum chamber). The results obtained for the second way are less sensitive on plasma neutron geometry. So, this way was used to anisotropy measurements.
- The research performed in this work confirmed the usefulness of the threshold nuclear reaction (e.g.  $^{115}\text{In}(n,n')^{115\text{m}}\text{In}$ ) to measure anisotropy of neutron emission from pinch plasma. It should be emphasized that the MCNP calculation ought to be used with the measurements in order to proper elaboration of neutron emission anisotropy.

## References

1. Bernstein MJ, Comisar GG (1972) Neutron energy and flux distributions from a crossed-field acceleration model of plasma focus and Z-pinch discharges. *Phys Fluids* 15:700–708
2. Bienkowska B, Karpinski L, Paduch M, Scholz M (2006) Measurements of neutron yield from PF-1000 device by activation method. *Czech J Phys* 56:B377–B382
3. Bienkowska B, Scholz M, Wincel K, Zareba B (2007) Use of activation technique and MCNP calculations for measurement of fast neutron spatial distribution at the MJ Plasma Focus device. In: *Proc of the Int Conf on Researches and Applications of Plasmas PLASMA 2007*, Greifswald, Germany, 1:349–352
4. Bronson FL, Venkataraman R (2000) Validation of the accuracy of the LabSOCS mathematical efficiency calibration for typical laboratory samples. In: *46th Annual Conf on Bioassay, Analytical and Environmental Radiochemistry*, 12–17 November 2000, Seattle, Washington, <http://www.canberra.com/pdf/Literature/LabSOC%20Accuracy%20Validation%20Paper.pdf>
5. Bronson FL, Young B, Venkataraman R (1998) Massetric efficiency calibrations of Ge detectors for laboratory applications. In: *44th Annual Conf on Bioassay, Analytical and Environmental Radiochemistry*, Albuquerque NM. <http://www.lanl.gov/BAER-Conference/BAERCon44p044.pdf>
6. Browne PF (1988) Pulsed particle beams in the plasma focus and in astrophysics. *J Phys D: Appl Phys* 21:596–602
7. Castillo F, Milanese, Moroso R, Pouzo J (1997) Some experimental research on anisotropic effects in the neutron emission of dense plasma-focus devices. *J Phys D: Appl Phys* 30:1499–1506
8. Gullickson RL, Luce JS, Sahlin HL (1977) Operation of a plasma-focus device with D2 and He3. *J Appl Phys* 48:9:3718–3722
9. Gullickson RL, Sahlin HL (1978) Measurements of high energy deuterons in the plasma focus device. *J Appl Phys* 49:3:1099–1115
10. [http://www.nndc.bnl.gov/nudat2/indx\\_dec.jsp](http://www.nndc.bnl.gov/nudat2/indx_dec.jsp)
11. Jednorog S, Scholz M, Popovichev M, Murari M, and JET EFDA contributors (2009) Numerical optimization of activation samples for the application of the activation technique to measure neutrons in large fusion devices like JET and ITER (abstract). In: *36th EPS Conf on Plasma Physics*, Sofia, Bulgaria: P2.152
12. Prokopowicz R, Bienkowska B, Drozdowicz K *et al.* (2011) Measurements of neutrons at JET by means of the activation methods. *Nucl Instrum Meth A* 637:119–127
13. Schmidt H, Kasperczyk A, Paduch M *et al.* (2002) Review of recent experiments with the megajoule PF-1000 plasma focus device. *Phys Scr* 66;2:168–1973
14. Scholz M, Bienkowska B, Chernyshova M *et al.* (2007) Fast-neutron source based on Plasma-Focus device. In: *Proc of the Int Conf on Researches and Applications of Plasmas PLASMA 2007*, Greifswald, Germany, 1:345–348
15. Steinmetz K, Hubner K, Rager JP, Robouch BV (1982) Neutron pinhole camera investigation on temporal and spatial structures of plasma focus neutron source. *Nucl Fusion* 22:30–33
16. Szydłowski A, Scholz M, Karpinski L, Sadowski M, Tomaszewski K, Paduch M (2001) Neutron and fast ion emission from PF-1000 facility equipped with new large electrodes. *Nukleonika* 46;Suppl 1:S61–S64
17. X-5 Monte Carlo Team (2003) MCNP – A General Monte Carlo N-Particle Transport Code
18. X-5 Monte Carlo Team (2003) MCNP5DATA: Standard Neutron Photoatomic, Photonuclear, and Electron Data Libraries for MCNP5, (CCC-710)